Texture Analysis for Classification of Cervix Lesions

Qiang Ji*, *Member, IEEE*, John Engel, and Eric Craine

***Abstract*—This paper presents a generalized statistical texture analysis technique for characterizing and recognizing typical, diagnostically most important, vascular patterns relating to cervical lesions from colposcopic images. The contributions of the research include: 1) the introduction of a generalized texture analysis technique based on the combination of the conventional statistical and structural textural analysis approaches by using a statistical description of geometric primitives; 2) the introduction of a set of textural measures that capture the specific characteristics of cervical textures as perceived by human. Experimental study with real images demonstrated the feasibility and promising of the proposed approach in discriminating between cervical texture patterns indicative of different stages of cervical lesions.**

***Index Terms*—Cervix lesion classification, colposcopic images, pattern recognition, texture analysis.**

I. Introduction

THE incidence of cervical cancer mortality has been dramatically reduced since the introduction of the Papanicolaou (Pap) smear test. However, the Pap test is unable to accurately and consistently identify premalignant and malignant disease of cervix. The incidence of both false-negative and false-positive test have become shockingly high [1]. These have motivated the use of colposcopy as a standard screening procedure for precancer examination [1] and for performing accurate punch biopsies for histological analysis. One of the major factors hindering the full utilization of colposcopy is the difficulty in training physicians in the recognition of pathology. Colposcopic images contain complex and confusing lesion patterns. Correctly analyzing and classifying different types of tissues require substantial training. It is, therefore, necessary to simplify the use of colposcopy and to enhance its capability so that average physicians can correctly recognize various tissue patterns in a consistent and uniform fashion. For this reason, we developed an image analysis system to help physicians better interpret various patterns on colposcopic images.

A careful examination of various cervical images reveals regular and repeatable vascular patterns, indicating different stages of dysplasia. In fact, vascular pattern is the most important diagnostic criteria used by colposcopists for recognizing pathology [2]. For example, two basic types of vascular patterns observable in normal or benign lesions are hairpin and network capillaries. On the other hand, different versions of punctation and mosaic vascular patterns may be observed in areas of dysplasia and carcinoma in situ. Fig. 1 pictorially shows typical vascular patterns encountered in cervical lesions.

We propose to recognize different vascular patterns of cervical lesions via a textural analysis. Various texture analysis methods have been developed to analyze and classify various tissue patterns including liver lesions [3], [4], prostrate cancerous lesions [5], brain tissue [6], clonic mucosa [7], mammographic tissue [8], and for segmentation of cardiac images [9]. However, *the use of texture analysis techniques (or other image processing approaches) for recognizing and classifying cervix lesions has not been reported in the literature to the best of our knowledge*.

Further examination of the textural patterns relating to cervical lesions revealed the following. First, texture patterns for cervical lesions are primarily due to the vascular patterns. The nonvascular structures in the cervical images contribute very little to the formation of texture patterns in cervical lesions. Furthermore, the vascular structures are mainly characterized by the geometric shape and spatial distribution of capillaries. The gray levels and thickness of capillaries are irrelevant to vascular patterns. Thus, cervix texture patterns cannot be characterized by the spatial intensity distribution of capillaries. Second, texture patterns for cervical lesions do not exhibit regular repetitive or periodic structures.

Based on the above observations, we proposed a novel generalized statistical method to characterize textural patterns of cervical lesions. Recognizing the fact that cervical textures are primarily represented by the vascular structures, we assume that a significant proportion of the texture information in cervix lesion is contained in the vascular structures. Our approach first extracts the vascular structures from the original cervical lesion images, followed by vectorizing the extracted vascular structure using line segments. Statistical distributions of the line segments (in terms of length and orientation) are then constructed. First- and second-order statistics derived from the joint and/or marginal distributions are used as textural measures for cervical lesions classification. The beauty of such a texture characterization is that while it takes full advantage of the traditional statistical textural analysis approach [10], it also inherents the power of the structural textural analysis by emphasizing the shape aspects of textures.

The rest of this paper is arranged as follows. In Section II, we discuss the propsoed algorithm. The results of experimental evaluation of the proposed algorithm are presented in Section III. The paper ends in Section IV with a summary.

Manuscript received December 15, 1998; revised August 16, 2000. This work was supported by a grant from the National Institutes of Health (NIH). The Associate Editor responsible for coordinating the review of this paper and recomending its publication was W. Higgins. *Asterisk indicates corresponding author*.

*Q. Ji is with the Department of Computer Science, University of Nevada Reno, NV 89557 USA (e-mail: qiangji@cs.unr.edu).

J. Engel and E. Craine are with Western Research Company, Tucson, AZ USA.

Publisher Item Identifier S 0278-0062(00)09740-8.

II. Algorithm Development

In this section, we detail our texture analysis technique for analyzing the textural patterns relating to cervical lesions. We discuss three aspects of the algorithm, namely, texture primitives extraction, statistical description of textural primitives, and textural metrics formulation and computation.

A. Texture Primitive Extraction

The proposed approach captures the cervical textural information by approximating the vascular structures using a set of connecting line segments. Texture primitive extraction is therefore concerned with extracting the line segments that approximate the vascular structures. This includes three steps: image preprocessing, skeletonization, and vectorization as discussed below.

Vascular structures often coexist with other irrelevant artifacts on the surface of a cervix. Furthermore, the presence of fluids and/or other discharges on cervix surface causes nonuniform luminance and contrast to the underlying vascular structures. Fig. 2(a) shows a colposcopic image of a portion of a cervix containing mosaic vascular pattern. The primary purpose of preprocessing is to digitally remove artifacts present on the surface of a cervix and to compensate the uneven luminance. Artifacts on the surface of a cervix image are identified and separated from the underlying vascular structures based on the morphological differences between artifacts and capillaries. The capillaries usually are much more tortuous than artifacts. Artifacts, on the other hand, are usually short and straight segments or small dots. The differences in morphology were exploited in separating them based on the theory of mathematical morphology. The technique of morphological opening with a rotating structure creates an image containing primarily artifacts, which are then subtracted from the original images, yielding images containing predominantly vascular structures. The rotating structure elements are necessary due to random orientations of the artifacts. Detailed description of this algorithm may be found in [11]. Non-uniform illumination is removed through background subtraction using the morphological rolling ball algorithm [12]. Fig. 2(b) shows an example of a morphologically enhanced image. The radius of the rolling ball varies depending on the vascular patterns being studied and image scales. For the examples shown in Fig. 2, a radius of three pixels was chosen.

Separating vascular structures from the image background is accomplished with an adaptive thresholding operation [13], resulting in a binary image as shown in Fig. 2(c) containing primarily vascular structures. Adaptive thresholding is chosen due to variations in local contrasts as shown in Fig. 2(b).

The binary images of vascular structures are subsequently skeletonized since we observed that vascular structures can be fully captured by their skeletons. We employed the thinning algorithm provided by Zhang [14]. With this algorithm, each capillary is thinned to a skeleton of unitary thickness. Fig. 3(a) shows the skeletonized image of the image in Fig. 2(c). The final step in primitive extraction involves vectorization to approximate the thinned vascular structures with connecting line segments via a variant of Hough transform (HT) we developed. Our HT differs from the standard in that it can detect line segments.

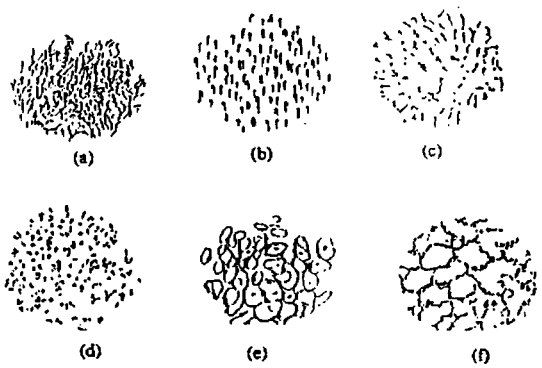

Fig. 1. Typical vascular patterns encountered in cervical lesions. (a) network capillaries in original squamous epithelium; (b) hairpin capillaries in original squamous epithelium; (c) and (d) punctation vessels in dysplasia and carcinoma in situ; and (e) and (f) mosaic vessels as seen in dysplasia and carcinoma *in situ*.

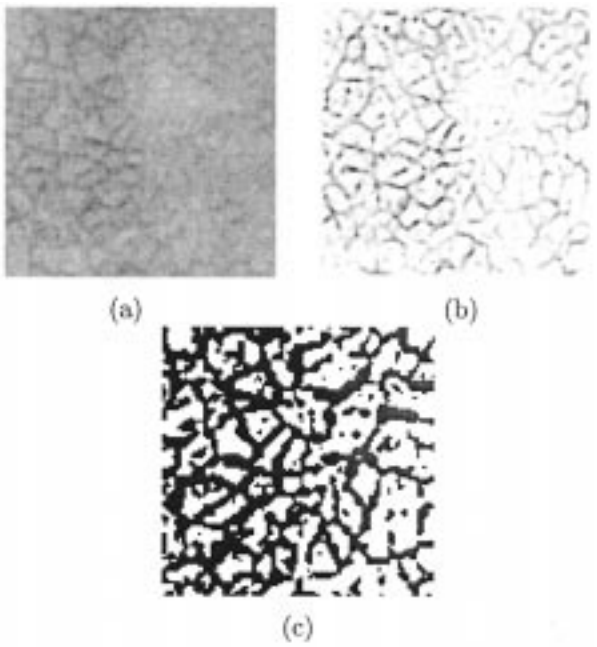

Fig. 2. (a) Original image containing mosaic patterns. (b) Morphologically enhanced image. (c) Binary image of (a) after adaptive thresholding of (b).

It consists of two steps: line segments detection and merging of short line segments. After merging, line segments shorter than a prespecified threshold are discarded. Fig. 3(b) shows the vectorized image of the image shown in Fig. 3(a).

B. Statistical Description of Textural Primitives

With texture primitives extracted, we have available a list of primitives (line segments) that model the vascular structures of the original image data. We need to proceed to the next phase of texture characterization–texture primitive attributes computation and their statistical distributions construction.

1) Statistical Distributions Construction: Since a line segment can be fully described by its length and orientation, line segment length and orientation are the natural choice of their properties. The properties of line segments can be treated as random variables and follow certain statistical distributions. We

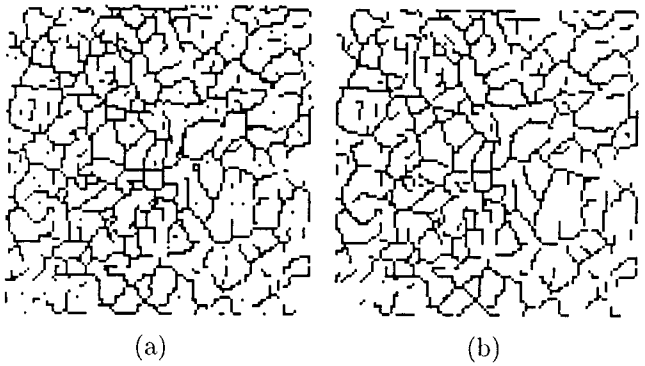

Fig. 3. (a) the skeletonized image of the image in Fig. 2(c); (b) the vectorized image of the image in (a). In (b), (a) is approximated by connecting line segments.

can construct statistical distributions for each vascular pattern. Since line segment length and orientation are of real values, discretization becomes necessary to study the statistical distributions of line segments. Discretization groups line segments into bins, based on their original values. Specifically, the orientations of line segments are uniformly discretized into 180 bins ranging from 0° to 179°. The line segment length is discretized in a similar fashion into L bins, where L was empirically selected as 50. After discretization, the length of each line segment is referred to by the number of the bin it belongs to rather than by its actual length.

With the attributes of line segments discretized, we can proceed to construct the density functions (histograms) of the line segments in terms of length and orientation. A total of three distributions were constructed for each pattern: one joint distribution and two marginal distributions. The joint distribution characterizes the line segment distribution by its length and orientation. Each point in the joint distribution represents the probability of a line segment with a particular length and orientation. The marginal distributions represent the line segment distribution with respect to length/orientation. Each point in a marginal distribution represents the probability of the line segment of a particular length (or orientation). Since line segments are of different lengths, the orientation distribution of line segments is therefore weighted by their lengths. This results in a more realistic orientation distribution. Fig. 4 shows the two marginal distributions of line segment length and orientation for the vectorized mosaic pattern shown in Fig. 3(b).

2) Distribution normalization: Since texture features are subsequently extracted from the above distributions, we need to ensure the invariance of the above distributions to affine image transformations, i.e., rotation, translation, and scale invariant. The normalization approach we followed needs to achieve only rotation invariance for orientation distribution since it is invariant to translation and scale. Similarly, for length distribution, only scale normalization is needed since it is invariant to translation and rotation.

The length distribution is normalized via discretization as discussed before. Since fixed discretization level (50) is used to discretize line segment length, scale only affects the discretization intervals. Given the fact that the lengths of the discretized line

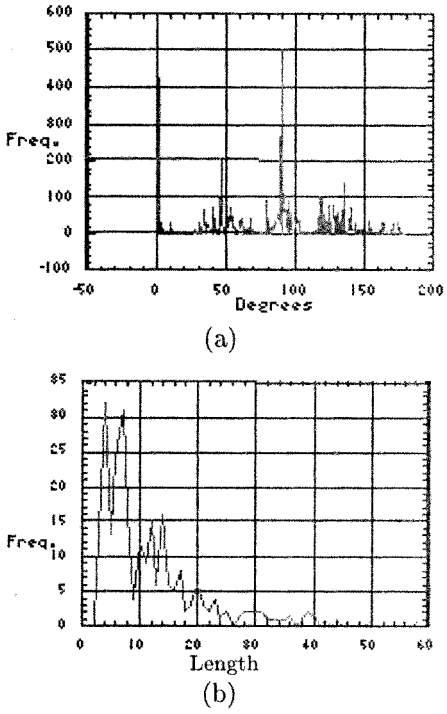

Fig. 4. Marginal probability density functions for orientation (a) and length (b) of the line segments in the vectorized mosaic pattern shown in Fig. 3(b).

segments are referred to by their bin numbers rather than by their actual lengths, the discretization makes the distribution independent of scale. For orientation distribution, a rotation (which is equivalent to adding or subtracting an angle to each line) may not only cause a linear shift for the interior bins (which may not affect the shape of the distribution) but also cause a circular shift for the boundary bins (bins close to 0 or 179) as shown in Fig. 5(a), where the local peak at 0° results from a circular shift of the corresponding local peak at about 140° in Fig. 4(a). This will alter the shape of original distribution, rendering incorrect feature values. Therefore, it must be normalized. The normalization is carried out as follows. Identify the peak of each distribution and shift the peak to the 90° bin and perform the same amount of shift for other angles. The choice of peak for normalization rather than other distribution marks like valley is because peak is less sensitive to noises. Fig. 5 shows the orientation distributions image with mosaics at two different orientations before and after normalization.

C. Texture Features Extraction

Most characteristic measurements characterizing the cervical lesion patterns are derived from the statistical distributions of the extracted line segments. They characterize the shapes of line segments distributions. Additional features are derived directly from the vectorized images to describe the spatial complexity and density (vascular concentration) of the texture patterns.

Efforts were made during feature extraction to select features that can relate to the specific textural characteristics of the cervical texture patterns. For example, some features relate to such textural characteristics as randomness, contrast, correlation etc., while others characterize the spatial complexity of the texture

patterns. We suggest a set of nine features which can be extracted from each of the two marginal distributions, four features from the joint distribution, and two features directly from the vectorized images, yielding a total of 24 features ($2 \times 9 + 4 + 2$). For illustrative purpose, we will define four of the 24 features in this section and explain their significance in relating to the specific characteristics of the cervical textures as perceived by human.

- *Peak density (f_1):* measures the strength of the local dominant peak in a marginal distribution, i.e., length or orientation distribution. $f_1 = \max(p(i))$ for $i = 1, 2, \ldots, N$, where $p(i)$ is the probability of the ith bin and N is the discretization level.
- *Entropy (f_7):* measures the randomness or homogeneity of a distribution with respect to length or orientation.
- *Ratio of the number of intersection points to the number of endpoints* (f_{14}): measures the spatial complexity of the textures
- *Density (f_{15})***:** measures the coarseness (or fineness) of a texture in terms of amount of edgels per unit area. The average number of edgels per unit area for all pixels is used as a measure of the density.

During feature design process, every effort was made to devise features that represent the specific characteristics of the cervical textures as perceived by human. Here, we will analyze some of the textural features we proposed and try to relate them to certain textural characteristics.

Peak density (f_1) measures the strength of the dominant length (or orientation) of line segment distribution with respect to a particular attribute. Take the orientation for example, hairpin texture pattern, with most line segments oriented in one direction as shown in Fig. 1, should have the highest f_1 (0.9) values among all cervical textural patterns while mosaics, with line segment directions scattering in all directions as shown in Fig. 1, should have the lowest (0.3). Similarly, for length distribution, hairpin texture pattern also has the highest peak density (0.8). Therefore, this feature can discriminate the mosaic and hairpin patterns.

Entropy (f_7) measures the randomness or homogeneity of a distribution with respect to length or orientation. Entropy takes a higher value for more random distribution. Take the orientation for example, Mosaics takes the highest value (1.2) while hairpin takes the lowest (0.5) value for the same reason as explained before. Therefore, this feature can discriminate the hairpin pattern from other patterns.

f_{14}, the ratio of number of intersection points to the number of endpoints (f_{14}) measures the spatial complexity of a texture. It takes a large value if capillaries interweave each other. For example, mosaics has the highest f_{14} value (1.3) while punctation takes the lowest (0.1). Furthermore, network pattern also has much higher value (0.8) than those of hairpin (0.3) and punctation. Therefore, this feature can discriminate mosaic and network patterns from others.

Density (f_{15}) measures the coarseness (or fineness) of texture in terms of amount of edgels per unit area. Coarse textures have a small number of edges per unit area while fine texture have a high number of edges per unit area. It measures the capillary concentration. For example, network pattern has the highest density (0.8) while punctation has the lowest density (0.2). Therefore, this feature can discriminate the network from punctation patterns.

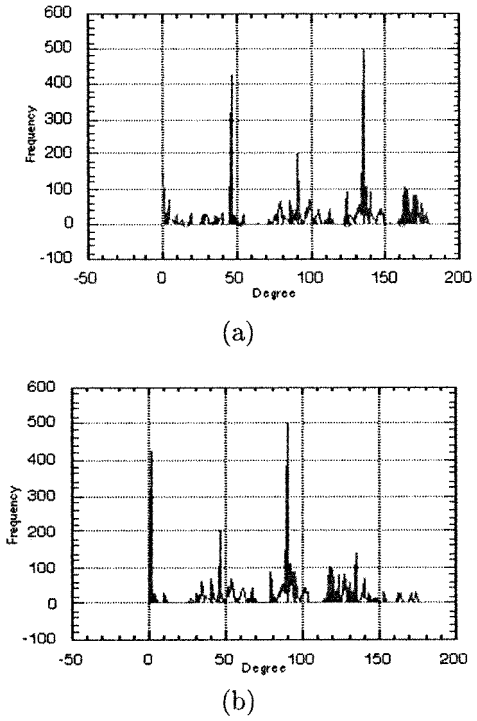

Fig. 5. The angle distributions of the mosaic image shown in Fig. 3(b) with and without normalization. (a) The angle distribution of the mosaic image with a 45-degree rotation (without normalization). (b) The angle distribution of (a) after normalization (its shape is very similar to that of Fig. 4(a)).

TABLE I
A SUBSET OF 13 OPTIMAL FEATURES

Joint Entropy
Angle Entropy
Angle Peak Ratio
Length Peak Density
Angle Peak Density
Length Entropy
#Intersections/#Ends
Info Entropy
Energy
Length Median
Angle Contrast
Length median/range

Other features used to describe the distributions include contrast, skewness, kurtosis, mean, median, correlation, and energy. A detailed definition of each feature may be found in [1].

D. Feature Analysis and Selection

An analysis of the extracted 24 features was conducted to study the effectiveness of each feature and to remove redundant features. One type of redundant features is features that are linearly correlated with each other. The linearly correlated features can be identified by computing the liner correlation coefficients between any two features. The identified correlated features are subsequently removed via feature pruning. Criterion used for

TABLE II
CLASSIFICATION RESULTS

	Mosaic 1	Mosaic 2	Puctation 1	Puctation 2	Network	Hairpin	% Correct
Mosaic 1	38 (31)	7 (6)	0 (0)	0 (0)	0 (8)	0 (0)	84.44 (68.88)
Mosaic 2	9 (9)	36 (36)	0 (0)	0 (0)	0 (0)	0 (0)	80.00 (80.00)
Puctation 1	0 (0)	0 (0)	35 (32)	10 (7)	0 (0)	0 (6)	77.77 (71.11)
Punctation 2	0 (0)	0 (0)	3 (0)	36 (38)	0 (0)	6 (7)	80.00 (84.44)
Network	0 (0)	0 (0)	0 (0)	0 (10)	45 (35)	0	100.00 (77.77)
Hairpin	0 (0)	0 (0)	0 (0)	0 (0)	0 (0)	45 (45)	100.00 (100.00)
Total	-	-	-	-	-	-	87.03 (80.36)

feature pruning include consistency, invariance, and discriminatory power. Consistency is measured by the within group variance, invariance measures features invariance to transformation, and discriminatory power determines a feature's discriminatory capability. Feature ranking rates the discriminatory power of each feature based on its capability in discriminating all classes. The ratio of between-class variance to the within group variance was used as a criterion. Analysis of the interclass and intraclass variance revealed some of the features to be ineffective, yielding a feature vector of reduced dimensionality.

III. EXPERIMENTAL EVALUATION

In this section, we present the preliminary results of our studies on the usefulness of the proposed texture features for categorizing a series of typical vascular patterns as shown in Fig. 1.

A. Image Acquisition and Feature Extraction

The experiment started with cervical image acquisition and preparation. The images to be prepared should contain the typical vascular pattern classes characterizing different stages of dysplasia. Typical vascular patterns to be recognized in this project include six vascular pattern classes as shown in Fig. 1.

To characterize each vascular pattern class accurately, 50 images were collected for each vascular pattern class, resulting in a total of 300 images. These images represent six classes. For each acquired image, we identified and marked a rectangular region corresponding to a known vascular pattern. The identified regions of interest were preprocessed. The preprocessed images were subsequently skeletonized and vectorized. The statistical distributions of line segments were then constructed, followed by the extraction of the 24 texture features. To perform feature selection, five images were randomly selected for each pattern class from the 300 images. Feature selection and analysis on the selected images yields 13 optimal features as shown in Table I.

B. Classification and Results

For classification, we employed the minimum-distance classifier. To train the classifier, we divided the remaining images (270) into two sets: one for testing and one for training. Due to the large feature vector dimension (24) and relatively smaller number of images (45 for each class pattern), cross-validation method was used for classification design and evaluation.

Specifically, for each training and testing session, 240 (40 for each class) sample images were used as the training data and the 30 (five for each class) left-out were used as the testing data. This process iterated nine times so that every sample image had the chance to be the left out and to be in the training set. The total number of correct classification over the nine iterations was used to evaluate the classification performance. For each testing, the minimum distance decision rule was used to classify the left-out image into one of six vascular pattern classes.

Two experiments were conducted. First, classification was performed using all 24 features. Second, the 13 optimal features defined in Table I were computed and used for classification. The performance of the classifier was recorded in the confusion matrix as shown in Table II.

The left most column of Table II is labeled with the actual classes, the top row shows the classified classes. The classification results using all 24 features are represented by the numbers outside parentheses while the numbers enclosed in parentheses represent the resultant output, using the optimal 13 features. In summary, we obtained the best discrimination performance (87.03%) by using all 24 features as shown in Table II. However, by using only the 13 optimal features resulting from feature ranking, our technique experiences a loss in classification accuracy (80.36%). The loss in accuracy seems to be minimal compared to the computational saving (almost 40%). Further experiments are needed to validate this.

IV. CONCLUSION

This paper describes a texture image analysis technique for characterizing and recognizing typical, diagnostically most important, vascular patterns relating to cervical lesions. We propose a generalized texture analysis technique based on combining the conventional statistical and structural approaches using a statistical description of geometric textural primitives. Preliminary experimental study demonstrated the feasibility of the proposed technique in discriminating between cervical texture patterns indicative of different stages of cervical lesions.

ACKNOWLEDGMENT

The authors would like to acknowledge the suggestions of the anonymous reviewers.

REFERENCES

[1] B. L. Craine, E. R. Craine, J. R. Engel, and N. T. Wemple, "A clinical system for digital imaging colposcopy," in *Proc. SPIE Medical Imaging II*, 1988, pp. 505–511.

[2] P. Kolstad and A. Stafl, *Atlas of Colposcopy*. Baltimore, MD: University Park, 1977.

[3] C. M. Wu and Y.-C. Chen, "Multi-threshold dimension vector for texture analysis and its application to liver tissue classification," *Pattern Recogn.*, vol. 26, no. 1, pp. 137–144, 1993.
[4] H. Sujana, S. Swarnamani, and S. Suresh, "Artificial neural networks for the classification of liver lesions by image texture parameters," *Ultrasound Med. Biol.*, vol. 22, no. 9, pp. 1177–1181, 1996.
[5] A. G. Houston and S. B. Premkumar, "Statistical interpretation of texture for medical applications," presented at the Proc. Biomedical Image Processing and Three Dimensional Microscopy, San Jose, 1991.
[6] F. Lachmann and C. Barillot, "Brain tissue classification from mri data by means of texture analysis," presented at the Proceedings of Medical Imaging VI: Image Processing, Newport Beach, CA, 1992.
[7] A. N. Esgiar, R. N. G. Naguib, B. S. Sharif, M. K. Bennett, and A. Murray, "Microscopic image analysis for quantitative measurement and feature identification of normal and cancerous colonic mucosa," *IEEE Trans. Inform. Technol. Biomed.*, vol. 2, pp. 197–203, Mar. 1998.
[8] C. Enderwick and E. Micheli-Tzanakou, "Classification of mammographic tissue using shape and texture features," in *Proc. 1997 19th Annu. Int. Conf. IEEE Engineering in Medicine and Biology Society*, 1997, pp. 810–813.
[9] C. Fortin and W. Ohley, "Automatic segmentation of cardiac images: Texture mapping," in *Proc. IEEE 17th Annu. Northeast Bioengineering Conf.*, Hartford, CT, 1991.
[10] R. M. Haralick, "Statistical and structural approaches to texture," in *Proceedings of Proc. IEEE*, 1979.
[11] B. D. Thackray and A. C. Nelson, "Semi-automatic segmentation of vascular network images using a rotating structuring element (rose) with mathematical morphology and dual feature thresholding," *IEEE Trans. Med. Imag.*, vol. 12, pp. 385–392, June 1993.
[12] S. Sternberg, "Biomedical image processing," *IEEE Comput. Mag.*, pp. 22–33, 1973.
[13] T. Kanade and K. C. Chow, "Boundary detection of radiographic images by a threshold method," *Frontiers Pattern Recogn.*, pp. 61–82, 1982.
[14] T. Y. Zhang and C. Y. Suen, "A fast parallel algorithm for thinning digital patterns," *Commun. ACM*, vol. 27, no. 3, pp. 236–239, 1984.